Hindawi Publishing Corporation
EURASIP Journal on Wireless Communications and Networking
Volume 2010, Article ID 835498, 11 pages
doi:10.1155/2010/835498

Research Article

Performance Analysis of Multibranch Dual-Hop Nonregenerative Relay Systems with EGC in Nakagami-m Channels

H. Q. Huynh,[1] S. I. Husain,[1] J. Yuan,[1] A. Razi,[1] and H. Suzuki[2]

[1] *School of Electrical Engineering and Telecommunications, The University of New South Wales, Sydney, NSW 2052, Australia*
[2] *Wireless Technologies Laboratory, CSIRO ICT Centre, Marsfield, NSW 2122, Australia*

Correspondence should be addressed to S. I. Husain, imtiaz_h_syed@yahoo.com

Received 16 July 2009; Revised 1 November 2009; Accepted 26 January 2010

Academic Editor: George Karagiannidis

The end-to-end performance of multibranch dual-hop wireless communication systems with nonregenerative relays and equal gain combiner (EGC) at the destination over independent Nakagami-m fading channels is studied. We present new closed form expressions for probability distribution function (PDF) and cumulative distribution function (CDF) of end-to-end signal to noise ratio (SNR) per branch in terms of Meijer's G function. From these results, analytical formulae for the moments of the output SNR, the average overall SNR, the amount of fading, and the spectral efficiency are also obtained in closed form. Instead of using moments-based approach to analyze the asymptotic error performance of the system, we employ the characteristic function (CHF) method to calculate the average bit error probability (ABEP) and the outage probability for several coherent and noncoherent modulation schemes. The accuracy of the analytical formulae is verified by various numerical results and simulations.

1. Introduction

Wireless relaying systems in which mobile terminals are employed to retransmit information from a source to a destination have attracted great attention as they can provide cooperative diversity [1, 2]. Exploiting the advantages of spatial diversity without the need of physical antenna arrays, the relaying systems can not only extend the coverage of microwave communications but also mitigate the effects of fading. In such systems, there are two typical kinds of relays. If the relay decodes the signal and transmits the decoded version to the destination, it is called a "regenerative" relay. On the other hand, if the relaying node just amplifies and retransmits the source signal to the next node, it is called a "non-regenerative" relay. Due to their simpler implementation, non-regenerative relay networks have been investigated more than any other relaying systems.

In the most recent literature, a lot of work has been done on the performance analysis of cooperative relay systems. In [3, 4], the end-to-end performance of one of branch dual-hop relaying systems operating in Rayleigh fading channels is analyzed. When the channels are characterized by generalized Nakagami-m fading, refernces [5, 6] propose mathematical methods to study the performance of a single relaying link system. Due to the use of only one relay, the diversity of these systems is limited. The performance of the relay system can be enhanced by utilizing many relays. In [7], the error performance of a multibranch dual-hop relay system in Rayleigh fading channels is studied. An asymptotic approach to analyze general cooperative links is introduced in [8]. The lower bound of the error performance of a cooperative dual-hop wireless system in Nakagami-m fading channels is derived in [9]. The common denominator in these papers is that the diversity combiner used at the receiver is the maximal ratio combiner (MRC). Therefore, the moment generating function (MGF) approach can be used to analyze the performance. However, the optimal MRC requires amplitude and phase estimates of the channel simultaneously. On the other hand, equal gain combining (EGC) offers a significant practical advantage because it provides performance comparable to MRC, but with much less complexity.

The performance of EGC has also been investigated by many researchers. In particular, a convergent infinite series for the complementary distribution function and the probability density function (PDF) of a sum of independent

random variables is derived in [10]. This series is then used to derive the bit error rate and the complementary distribution function of the SNR at the output of an L-branch EGC system [11]. A characteristic function (CHF) approach to study the performance of EGC over Rayleigh channels is proposed in [12–14]. This idea was later extended to compute the average symbol error rate of a broad class of modulation schemes in different fading environments [15, 16]. A moments-based approach to calculate the performance of equal gain diversity is presented in [17, 18]. This method employs the Padé approximants to approximate the truncated series of MGF from which the average bit error probability (ABEP) and the outage probability P_{out} are obtained. However, to the best of authors' knowledge, there is no published work on the performance of L-branch dual-hop cooperative systems with non-regenerative relays and EGC at the receiver. The reason is that the derivation of the distribution of the sum of relaying branch envelopes is a very difficult task.

In this paper, we focus on multibranch dual-hop non-regenerative relay systems working in slow and flat Nakagami-m environments. Among the nonselective fading models, Nakagami distribution is the most flexible because it does not only match the bulk of empirical data, but also includes the Rayleigh and one-sided Gaussian distributions as special cases. Using a special function, Meijer's G function, we provide an alternative expression for the PDF of end-to-end SNR. This is the key contribution of this paper, from which we can derive some important performance parameters such as moments of the overall SNR, amount of fading (AoF), and spectral efficiency (SE) in closed form expressions. Once the closed form formulae of the moments of SNR are obtained, we can use the moments-based approach to compute the approximate performance of the relay system. However, to get expressions for the ABEP and P_{out}, we employ the CHF method as in [12, 13, 16]. The main contributions of this paper include the following: (a) derivation of closed form formulae for the moments of the overall SNR, (b) derivation of the CHF of the fading envelope, which can be expressed in product and polar forms, (c) derivation of the analytical expressions for the ABEP for coherent and noncoherent schemes, and (d) evaluation of the outage probability of the system in terms of one integral, which can be computed easily.

The remainder of the paper is organized as follows. We first illustrate the relay system and the channel model in Section 2. The average probability statistics, APEB, and P_{out} are derived in Section 3. Some typical numerical and simulation results are presented in Section 4. Finally, Section 5 concludes the paper.

2. System and Channel Model

A cooperative system is considered in which a source node transmits signals to a destination node with the help of L intermediate relay nodes, as shown in Figure 1. We assume that all the channels used for information transmission in this system are orthogonal to each other. The source first broadcasts the signal to the destination and the L relays. The ith relay then amplifies the received signal and forwards it to the destination. Let s be the transmitted symbol with energy per symbol E_s, the baseband signal received at the destination directly from the source is

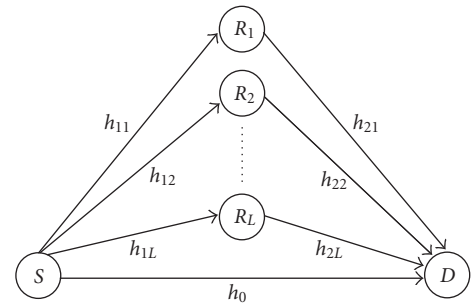

Figure 1: A multibranch dual-hop relay system with L relay nodes.

$$y_{D0} = h_0 s + n_0, \tag{1}$$

where h_0 and n_0 are the fading factor and the noise of the direct link, respectively. Similarly, the received baseband signal at the destination via the ith relay can be given as

$$y_{Di} = h_{2i}\{g_i(h_{1i}s + n_{1i})\} + n_{2i}, \tag{2}$$

where h_{1i}, h_{2i} and n_{1i}, n_{2i} are the fading factors and the noise samples of the first and second hops of the ith branch, respectively. The amplifying factor of the ith node is g_i. In this paper, we assume that n_0, n_{1i}, and n_{2i} are independent and identically distributed (i.i.d) complex Gaussian random variables (RVs) with the same single-sided power spectral density N_0. The fading factors h_0, h_{1i}, and h_{2i} follow slow and flat Nakagami-m fading, that is, their amplitudes have a central chi-squared distribution as in [19, (2.20)]

$$p_{|h|}(|h|) = \frac{2m^m|h|^{2m-1}}{\Omega^m\Gamma(m)}\exp\left(-\frac{m|h|^2}{\Omega}\right), \tag{3}$$

where m is the Nakagami-m fading parameter related to fading severity ($m \geq 0.5$), $\Omega = \mathbf{E}(|h|^2)$, $\mathbf{E}$ is the expectation operator, and $\Gamma(\cdot)$ is the Gamma function defined in [20, 8.310] . Furthermore, we assume that the fading characteristics among relay branches are independent. For the simplicity of the analysis, we assume that the fading parameters of the first and the second hops in the same branch are taken to be identical, that is, $m_{1i} = m_{2i}$ and $\Omega_{1i} = \Omega_{2i}$.

The end-to-end signal-to-noise ratios (SNR_{end}) of the direct transmission and the ith branch are

$$\gamma_0 = \frac{|h_0|^2E_s}{N_0}, \tag{4}$$

$$\gamma_i = \frac{g_i^2|h_{2i}|^2|h_{1i}|^2E_s}{\left(1 + g_i^2|h_{2i}|^2\right)N_0}. \tag{5}$$

Assume that the relay node is able to estimate the channel state information (CSI) in the first hop, the amplifying gain g_i of the ith relay is then chosen as

$$g_i = \frac{1}{\sqrt{|h_{1i}|^2 + N_0}} \approx \frac{1}{|h_{1i}|}. \tag{6}$$

Due to transmission power constraints, we want retransmissions to have the same power. The above choice of amplifying gain g_i will invert the fading effect of the first hop and the retransmitted signals from the relays will have the same power. Replacing (6) in (5), the SNR_{end} of the ith branch can be written as

$$\gamma_i = \frac{\gamma_{1i}\gamma_{2i}}{\gamma_{1i} + \gamma_{2i}}, \tag{7}$$

where $\gamma_{1i} = |h_{1i}|^2 E_s/N_0$ and $\gamma_{2i} = |h_{2i}|^2 E_s/N_0$. As $|h_0|, |h_{1i}|$ and $|h_{2i}|$ have Nakagami-m distribution, the individual SNRs γ_0, γ_{1i} and γ_{2i} will have Gamma distribution [19, (2.21)]

$$p_\gamma(\gamma) = \frac{m^m \gamma^{m-1}}{\overline{\gamma}^m \Gamma(m)} \exp\left(-\frac{m\gamma}{\overline{\gamma}}\right), \tag{8}$$

where $\overline{\gamma} = \Omega E_s/N_0$. Since γ_0 represents the end-to-end SNR of the direct link, $p_{\gamma_0}(\gamma_0)$ has the same distribution as $p_\gamma(\gamma)$, that is,

$$p_{\gamma_0}(\gamma_0) = \frac{m_0^{m_0} \gamma^{m_0-1}}{\overline{\gamma_0}^{m_0} \Gamma(m_0)} \exp\left(-\frac{m_0\gamma_0}{\overline{\gamma_0}}\right). \tag{9}$$

The end-to-end SNR of the ith relay branch has the form of the half harmonic mean of two i.i.d Gamma RVs, its PDF is derived in [5, Appendix A] as

$$p_{\gamma_i}(\gamma_i) = \frac{2^{\alpha_i}\sqrt{\pi}\gamma_i^{(3\alpha_i-3)/2}}{\beta_i^{(3\alpha_i-1)/2}\Gamma^2(\alpha_i)} \exp\left(-\frac{2\gamma_i}{\beta_i}\right) W_{\alpha_i/2,-\alpha_i/2}\left(\frac{4\alpha_i}{\beta_i}\right), \tag{10}$$

where $W(\cdot)$ is the Whittaker function defined in [20, (9.222)], $\alpha_i = m_i$, and $\beta_i = \overline{\gamma}_i/m_i$. Here, by applying the formula in [21, page 442], we can rewrite (10) in terms of Meijer's G function as

$$p_{\gamma_i}(\gamma_i) = A_i G_{1,2}^{2,0}\left(\lambda_i\gamma_i \middle|_{m_i-1,2m_i-1}^{m_i-1/2}\right), \tag{11}$$

where we denote

$$A_i = \frac{m_i\sqrt{\pi}}{\overline{\gamma}_i \cdot 2^{2m_i-3} \cdot \Gamma^2(m_i)}, \qquad \lambda_i = \frac{4m_i}{\overline{\gamma}_i}, \tag{12}$$

with $m_i = m_{1i} = m_{2i}$, $\overline{\gamma}_i = \overline{\gamma}_{1i} = \overline{\gamma}_{2i}$ and $G(\cdot)$ is Meijer's G function defined in [20, (9.301)]. With the help of [22, (26)], the corresponding cumulative distribution function (CDF) of γ_i is evaluated in closed form as

$$P_{\gamma_i}(\gamma_i) = A_i\gamma_i G_{2,3}^{2,1}\left(\lambda_i\gamma_i \middle|_{m_i-1,2m_i-1,1}^{0,m_i-1/2}\right). \tag{13}$$

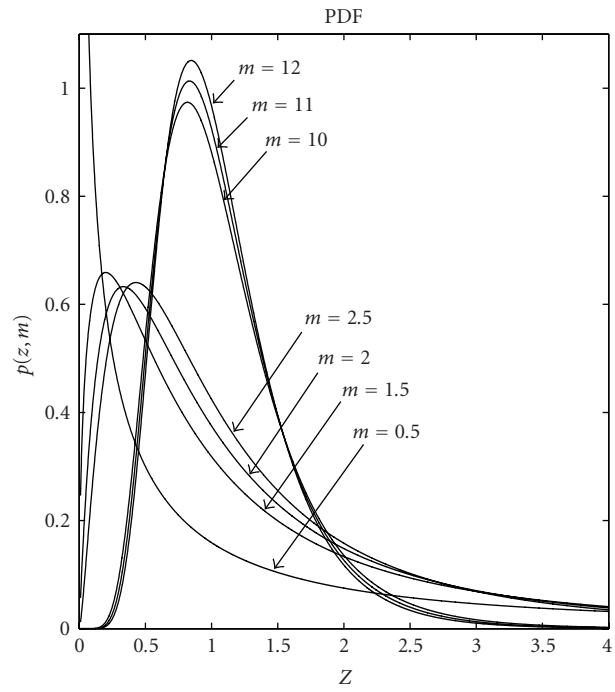

Figure 2: PDF of Z with different values of m.

In this paper, the EGC combiner is employed at the receiver. The output of various branches is first cophased and weighted equally before being summed to provide the total output. The overall SNR at the output of the EGC combiner is

$$\gamma_{\text{EGC}} = \frac{E_s\left(|h_0| + \sum_{i=1}^{L}|h_{2i}| \cdot g_i \cdot |h_{1i}|\right)^2}{N_0\left[1 + \sum_{i=1}^{L}\left(1 + |h_{2i}|^2 g_i^2\right)\right]}. \tag{14}$$

Substituting $g_i = 1/|h_{1i}|$, γ_{EGC} can be written as

$$\gamma_{\text{EGC}} = \frac{E_s\left(|h_0| + \sum_{i=1}^{L}|h_{2i}|\right)^2}{N_0\left[1 + \sum_{i=1}^{L}\left(1 + |h_{2i}|^2/|h_{1i}|^2\right)\right]}. \tag{15}$$

Due to the presence of $|h_{2i}|^2/|h_{1i}|^2$ in the denominator, the above form of γ_{EGC} is mathematically intractable. A more simpler expression is required for further analysis.

With the assumption that $|h_{1i}|$ and $|h_{2i}|$ have the same fading parameters, that is, $m_i = m_{1i} = m_{2i}$ and $\Omega_i = \Omega_{1i} = \Omega_{2i}$, we define the term $|h_{2i}|^2/|h_{1i}|^2$ in the denominator of (15) as a new RV, Z_i, whose PDF is independent of Ω_i. The PDF of Z_i is given by

$$p_{Z_i}(z_i) = \frac{\Gamma(2m_i)}{\Gamma^2(m_i)} \cdot \frac{z_i^{m_i-1}}{(1+z_i)^2 m_i}. \tag{16}$$

Its mean and variance are $m_i/(m_i - 1)$ and $m_i(2m_i - 1)/(m_i - 2)(m_i - 1)^2$, respectively. For proof see Appendix A.

The PDFs of Z_i with different values of m_i are plotted in Figure 2. It shows that the PDF of Z_i only depends upon m_i. It is clear from the figure that the PDFs tend to acquire similar

shapes for larger values of m_i. Therefore, if $m_i = m$, for all $i \in \{0, 1, \ldots, L\}$ or all values of m_i being large, all the signal branches will experience similar fading. Eventually, the noise characteristics in each branch would be the same, except the direct link due to single-hop transmission. Hence, including the direct link, the total noise term is roughly $L + 1$ times the multiple of N_0. An appropriate scaling or normalization of the noise leaves only $L + 1$ in the denominator. The received signal amplitude from each relay can be approximated as the square root of the received SNR which absorbs N_0 in it. A similar approximation is also used in [23]. It leads to the fact that instantaneous output SNR of EGC can be approximated as [23]

$$\gamma_{\mathrm{EGC}} \approx \frac{\left(\sum_{i=0}^{L} \sqrt{\gamma_i}\right)^2}{L+1}. \tag{17}$$

3. Performance Analysis

3.1. Moments of Output SNR. In this section, we derive closed form expression for the moments of output SNR. Once this formula becomes available, we can evaluate the average output SNR, the amount of fading, and the spectral efficiency of the relay system.

Using (17), the nth moment of the EGC output SNR is defined as

$$\mu_n^{\mathrm{EGC}} = \mathbf{E}[\gamma_{\mathrm{EGC}}^n] = \frac{1}{(1+L)^n}\mathbf{E}\left[\left(\sum_{i=0}^{L}\sqrt{\gamma_i}\right)^{2n}\right]. \tag{18}$$

Expanding the argument of the expectation operator in the above using multinomial identity in [22, 24.1.2] , we get

$$\mu_n^{\mathrm{EGC}} = \frac{(2n)!}{(1+L)^n}\mathbf{E}\left[\sum_{\substack{k_0,\ldots,k_L=0 \\ k_0+\cdots+k_L=2n}}^{2n} \frac{\gamma_0^{k_0/2}\cdots\gamma_L^{k_{L/2}}}{k_0!\cdots k_L!}\right]. \tag{19}$$

Let the input signals to the EGC be uncorrelated, in this case the mean product in (19) can be expressed as a product of the means, as given below

$$\mu_n^{\mathrm{EGC}} = \sum_{\substack{k_0,\ldots,k_L=0 \\ k_0+\cdots+k_L=2n}}^{2n} \left(\prod_{i=0}^{i=L}\frac{\mathbf{E}\left[\gamma_i^{k_i/2}\right]}{k_i!}\right). \tag{20}$$

Each term in (20) can be obtained as below

For the direct link having Nakagami-m distribution, the moment of γ_0 is

$$\mathbf{E}\left[\gamma_0^{k_0/2}\right] = \frac{\Gamma(m_0 + k_0/2)}{\Gamma(m_0)}\left(\frac{\overline{\gamma}_0}{m_0}\right)^{k_0/2}. \tag{21}$$

For the relaying link, the moment of γ_i can be derived from the definition

$$\begin{aligned}\mathbf{E}\left[\gamma_i^{k_i/2}\right] &= A_i\int_0^\infty \gamma_i^{k_i/2} G_{1,2}^{2,0}\left(\lambda_i\gamma_i\middle|_{m_i-1,2m_i-1}^{m_i-1/2}\right)d\gamma_i \\ &= \frac{A_i}{\lambda_i^{k_i/2+1}}\frac{\Gamma(m_i + k_i/2)\Gamma(2m_i + k_i/2)}{\Gamma(m_i + k_i/2 + 1/2)}.\end{aligned} \tag{22}$$

The integral in (22) is obtained using [20, 7.811.4] . Substituting (21) and (22) in (20), we get the moment of the output SNR of the EGC in the closed form as

$$\begin{aligned}\mu_n^{\mathrm{EGC}} = {} & \frac{(2n)!}{(1+L)^n} \\ & \times \sum_{\substack{k_0,\ldots,k_L=0 \\ k_0+\cdots+k_L=2n}}^{2n}\left[\frac{\Gamma(m_0 + k_0/2)}{k_0!\Gamma(m_0)}\left(\frac{\overline{\gamma}_0}{m_0}\right)^{k_0/2} \times \prod_{i=1}^{L}\frac{A_i}{k_i!\lambda_i^{k_i/2+1}}\right. \\ & \left. \times\frac{\Gamma(m_i + k_i/2)\Gamma(2m_i + k_i/2)}{\Gamma(m_i + k_i/2 + 1/2)}\right].\end{aligned} \tag{23}$$

3.1.1. Average Output SNR. As the receiver employs EGC with independent input branches, the average output SNR, after some mathematical manipulations, can be obtained in the closed form by setting $n = 1$ in (23) as

$$\overline{\gamma}_{\mathrm{EGC}} = \frac{1}{1+L}\left[\sum_{i=0}^{L}\overline{\gamma}_i + 2\sum_{i=1}^{L}\sum_{j=0}^{i-1}\overline{\gamma_i^{1/2}}\ \overline{\gamma_j^{1/2}}\right], \tag{24}$$

where $\overline{\gamma_i^{1/2}}$ and $\overline{\gamma_j^{1/2}}$ can be found from (21) and (22) by putting $k_0 = k_i = 1$.

3.1.2. Amount of Fading (AoF). The amount of fading (AoF) or fading figure associated with the fading PDF is defined as a measure of the severity of the fading and is typically independent of the average fading power. Mathematically, it can be defined as

$$\mathrm{AoF} = \frac{\mathrm{var}(\gamma_{\mathrm{EGC}})}{\left(\mathbf{E}[\gamma_{\mathrm{EGC}}]\right)^2} = \frac{\mu_2^{\mathrm{EGC}}}{\overline{\gamma}_{\mathrm{EGC}}^2} - 1, \tag{25}$$

where $\mathrm{var}(\gamma_{\mathrm{EGC}})$ is the variance of the EGC output SNR. From (23) with $n = 2$ and (24), the AoF of the EGC receiver operating Nakagami-m fading channels is obtained as

AoF

$$= \frac{4!\sum^{4}_{\substack{k_0,\ldots,k_L=0\\ k_0+\cdots+k_L=4}} \left[\left(\Gamma(m_0+k_0/2)/k_0!\Gamma(m_0)\right)\left(\overline{\gamma}_0/m_0\right)^{k_0/2}\prod_{i=1}^{L}\left(A_i/k_i!\lambda_i^{k_i/2+1}\right)\left(\Gamma(m_i+k_i/2)\Gamma(2m_i+k_i/2)/\Gamma(m_i+k_i/2+1/2)\right)\right]}{\left[\sum_{i=0}^{L}\overline{\gamma}_i + 2\sum_{i=1}^{L}\sum_{j=0}^{i-1}\overline{\gamma_i^{1/2}\ \gamma_j^{1/2}}\right]^2} - 1. \tag{26}$$

3.1.3. Spectral Efficiency (SE). The AoF can be used to study the spectral efficiency (SE) of a flat fading channel in a very noisy region. In this low power region, it is easy to see that the minimum bit energy over noise level required for reliable communication is −1.59 dB. The slope of the SE versus E_s/N_0 in b/s/Hz per 3 dB at $(E_s/N_0)_{\min}$ is

$$S_0 = \frac{2\left(\mathbf{E}[a^2]\right)^2}{\mathbf{E}[a^4]} = \frac{2\overline{\gamma}^2_{\mathrm{EGC}}}{\mu_2^{\mathrm{EGC}}}, \tag{27}$$

where a is the EGC output amplitude. Substituting (25) in (27), the slope of the SE in a very noisy region can be expressed in a useful form as

$$S_0 = \frac{2}{\mathrm{AoF}+1}. \tag{28}$$

3.2. Average Bit Error Probability (ABEP). After evaluating the moment of the EGC output SNR in a closed form, the moments-based approach [17] can be applied to evaluate the performance of the considered system with the EGC in Nakagami-m fading channels. However, this method can only provide asymptotic measures for ABEP and P_{out} because of the truncation in Padé approximation. Due to the compact form PDF of γ_i in (11), the approaches in [12, 16] can be used. These methods basically exploit Gil-Palaez's Lemma 1 to get the exact expressions for ABEP and P_{out}.

3.2.1. For Coherent Detection (BPSK, BFSK). The ABEP for coherent detection such as binary phase shift keying (BPSK) and binary frequency shift keying (BFSK) has a generic form in terms of Gaussian Q function as

$$\overline{P}_e = \mathbf{E}\left[Q\left(\sqrt{2g\gamma_{\mathrm{EGC}}}\right)\right] = \mathbf{E}\left[Q\left(\sqrt{G}r\right)\right], \tag{29}$$

where $G = 2g/(1+L)$ with $g = 1$ and 0.5 for coherent BPSK and BFSK, respectively, and $r = \sum_{i=0}^{L} r_i$ with $r_i = \sqrt{\gamma_i}$. The PDFs of r_i can be derived using the PDFs of γ_0 and γ_i in (9) and (11), respectively. For proof see Appendix B

$$\begin{aligned} p_{r_0}(r_0) &= 2A_0 r_0^{2m_0-1}\exp\left(-\frac{m_0}{\overline{\gamma}_0}r_0^2\right),\\ p_{r_i}(r_i) &= 2A_i r_i G_{1,2}^{2,0}\left(\lambda_i r_i^2 \,\middle|\, {m_i-1/2 \atop m_i-1,2m_i-1}\right). \end{aligned} \tag{30}$$

To obtain the error performance, the CHF of the decision variable r is considered. By definition, the CHF of r is given by

$$\phi_r(t) = \mathbf{E}[\exp(jrt)] = \int_0^\infty e^{jrt} p_r(r)(t)dt. \tag{31}$$

Based on the assumption that all the input signals through different branches are mutually uncorrelated, we get the CHF of r as

$$\phi_r(t) = \phi_{r_0}(t)\prod_{i=1}^{L}\phi_{r_i}(t), \tag{32}$$

where $\phi_{r_0}(t)$ and $\phi_{r_i}(t)$ are the CHFs of the direct and the ith branch, respectively. By substituting $p_{r_0}(r_0)$ from (30) to (31), the value of $\phi_{r_0}(t)$ can be obtained in terms of Meijer's G function. See Appendix C for proof

$$\phi_{r_0}(r_0) = \Phi_0^*\left[c_0(t) + j\,\mathrm{sign}(t)d_0(t)\right], \tag{33}$$

where

$$\begin{aligned} \Phi_0^* &= \frac{\sqrt{\pi}}{\Gamma(m_0)},\\ c_0(t) &= G_{1,2}^{1,1}\left(\frac{\overline{\gamma}_0 t^2}{4m_0}\,\middle|\, {1-m_0 \atop 0,1/2}\right),\\ d_0(t) &= G_{1,2}^{1,1}\left(\frac{\overline{\gamma}_0 t^2}{4m_0}\,\middle|\, {1-m_0 \atop 1/2,0}\right), \end{aligned} \tag{34}$$

and $\mathrm{sign}(\cdot)$ is the sign function. Similarly, by using the PDF of r_i in (30), CHF of r_i can also be determined in terms of Meijer's G function. Proof can be seen in Appendix C

$$\phi_{r_i}(r_i) = \Phi_i^*\left[c_i(t) + j\,\mathrm{sign}(t)d_i(t)\right], \tag{35}$$

where

$$\begin{aligned} \Phi_i^* &= \frac{2\pi}{\left[4^{m_i}\Gamma^2(m_i)\right]},\\ c_i(t) &= G_{2,3}^{1,2}\left(\frac{t^2}{4\lambda_i}\,\middle|\, {1-m_i,1-2m_i \atop 0,1/2-m_i,1/2}\right),\\ d_i(t) &= G_{2,3}^{1,2}\left(\frac{t^2}{4\lambda_i}\,\middle|\, {1-m_i,1-2m_i \atop 1/2,1/2-m_i,0}\right). \end{aligned} \tag{36}$$

Substituting (33) and (35) in (32), we can rewrite $\phi_r(t)$ in the product form as

$$\phi_r(t) = \prod_{i=0}^{L}\Phi_i^*\left[c_i(t) + jd_i(t)\right], \tag{37}$$

or in a polar form as

$$\phi_r(t)=\prod_{i=0}^{L}\Phi_i^*\left[c_i^2(t)+d_i^2(t)\right]^{1/2}\exp\left(j\sum_{i=0}^{L}\tan^{-1}\left[\frac{\text{sign}(t)d_i(t)}{c_i(t)}\right]\right). \tag{38}$$

After getting the CHF of the decision variable, its PDF can be determined by taking inverse Fourier transform and eventually the ABEP can be evaluated. It is obvious that evaluating the inverse Fourier integral is not an easy task. Therefore, we exploit the relationship between the CHF and its CDF in order to measure the exact ABEP of coherent detection. This expression was derived by Gil-Palaez in 1951, which is restated here for convenience.

Lemma 1 (Gil-Palaez]). *Let $F(x)$ be a one-dimensional CDF and let $\phi(t)$ be the corresponding CHF with a real variable t, then*

$$F(x)=\frac{1}{2}-\frac{1}{\pi}\int_0^{\infty}\frac{\text{Im}[\phi(t)e^{-jtx}]}{t}dt, \tag{39}$$

where $\text{Im}(\cdot)$ *denotes the imaginary part.*

Using this lemma and an alternative exponential integral formula for the Gaussian Q function [24, (14b)], the ABEP can be written in terms of the CHF of r as in [16, (3)]

$$\overline{P}_e=\frac{1}{2}-\frac{1}{\pi}\int_0^{\infty}\frac{\text{Im}[\phi_r(\sqrt{2Gt})]}{te^t}dt. \tag{40}$$

By substituting (37) in (40), the ABEP for coherent detection can be represented in a product-sum integral form. For the case $L=1$, the ABEP is given by

$$\overline{P}_e=\frac{1}{2}-\frac{\Phi_0^*\Phi_1^*}{2\pi}\int_0^{\infty}\frac{c_0(t')d_1(t')+c_1(t')d_0(t')}{te^t}\,dt, \tag{41}$$

where $t'=\sqrt{2Gt}$. For the two-branch system, the ABEP is

$$\begin{aligned}\overline{P}_e=&\frac{1}{2}-\frac{\Phi_0^*\Phi_1^*\Phi_2^*}{2\pi}\\&\times\int_0^{\infty}[c_0(t')c_1(t')d_2(t')+c_0(t')c_2(t')d_1(t')\\&\quad+c_1(t')c_2(t')d_0(t')\\&\quad-d_0(t')d_1(t')d_2(t')]\frac{dt}{te^t}.\end{aligned} \tag{42}$$

Similarly, substituting (38) in (40), we derive the ABEP as

$$\begin{aligned}\overline{P}_e=&\frac{1}{2}-\frac{\prod_{i=0}^{L}\Phi_i^*}{2\pi}\\&\times\int_0^{\infty}\prod_{i=0}^{L}\left[c_i^2(t')+d_i^2(t')\right]^{1/2}\sin\left(\sum_{i=0}^{L}\tan^{-1}\frac{d_i(t')}{c_i(t')}\right)\frac{dt}{te^t}.\end{aligned} \tag{43}$$

Though the above result is not in the closed form; however, it is useful for the ABEP because it involves only one-fold integral which can be evaluated using any numerical integration technique or software.

3.2.2. For Noncoherent Detection (DBPSK, NCFSK). For noncoherent detection, the ABEP has a generic formula as

$$\overline{P}_e=\mathbf{E}[0.5\exp(-g^*\gamma_{\text{EGC}})]=\mathbf{E}[0.5\exp(-G^*r^2)], \tag{44}$$

with $g^*=1$ and 0.5 for DBPSK and NCFSK, respectively, and we set $G^*=g^*/(L+1)$. By expressing the PDF of r in terms of $\phi_r(t)$ and rearranging the integral order, we obtain the ABEP as in [13, (26)]

$$\overline{P}_e=\frac{1}{4\pi}\int_{-\infty}^{\infty}\phi_r(t)\int_0^{\infty}e^{-G^*r^2}e^{-jrt}dr\,dt. \tag{45}$$

The inner integral can be derived from [20, (3.896)], from which we can express $\overline{P}_e$ as a sum of integrals

$$\begin{aligned}\overline{P}_e=&\frac{1}{8\sqrt{\pi G^*}}\int_{-\infty}^{\infty}\phi_r(t)e^{-t^2/4G^*}dt\\&-\frac{j}{8\pi G^*}\int_{-\infty}^{\infty}{}_1F_1\left(1;\frac{3}{2};-\frac{t^2}{4G^*}\right)t\phi_r(t)dt,\end{aligned} \tag{46}$$

where ${}_1F_1(\cdot)$ is the confluent hypergeometric function defined in [20, 9.14.1] . Since the functions $c_i(t)$ and $d_i(t)$ are even, the expression for ABEP can be further simplified. For example, in case of $L=1$, using the product form of CHF of r given in (37), the above expression can be written as

$$\begin{aligned}\overline{P}_e=&\frac{\Phi_0^*\Phi_1^*}{4\sqrt{\pi G^*}}\int_0^{\infty}[c_0(t)c_1(t)-d_0(t)d_1(t)]e^{-t^2/4G^*}dt\\&+\frac{\Phi_0^*\Phi_1^*}{4\pi G^*}\int_0^{\infty}[c_0(t)d_1(t)+c_1(t)d_0(t)]\\&\qquad\times{}_1F_1\left(1;\frac{3}{2};-\frac{t^2}{4G^*}\right)t\,dt.\end{aligned} \tag{47}$$

In case of two branches, that is, $L=2$, the ABEP becomes

$$\begin{aligned}\overline{P}_e=&\frac{\Phi_0^*\Phi_1^*\Phi_2^*}{4\sqrt{\pi G^*}}\\&\times\int_0^{\infty}[c_0(t)c_1(t)c_2(t)-c_0(t)d_1(t)d_2(t)\\&\qquad-c_1(t)d_0(t)d_2(t)-c_2(t)d_0(t)d_1(t)]e^{-t^2/4G^*}dt\\&+\frac{\Phi_0^*\Phi_1^*\Phi_2^*}{4\pi G^*}\\&\times\int_0^{\infty}[c_0(t)c_1(t)d_2(t)+c_0(t)c_2(t)d_1(t)\\&\qquad+c_1(t)c_2(t)d_0(t)-d_0(t)d_1(t)d_2(t)]\\&\qquad\times{}_1F_1\left(1;\frac{3}{2};-\frac{t^2}{4G^*}\right)t\,dt.\end{aligned} \tag{48}$$

These formulae can be easily used to calculate the ABEP in noncoherent signal detection with EGC at the receiver. In the simulation results presented in Section 4, these integrals are evaluated using Mathematica software.

3.2.3. Outage Probability P_{out}. Setting γ_{th} as a specific threshold, the outage probability is defined as the probability that the output SNR γ_{EGC} falls below γ_{th}, that is,

$$\begin{aligned} P_{\text{out}} &= P(\gamma_{\text{EGC}} \le \gamma_{\text{th}}) \\ &= P\left(\frac{\left(\sum_{i=0}^{L}\sqrt{\gamma_i}\right)^2}{L+1} \le \gamma_{\text{th}}\right) \\ &= P\left(\sum_{i=0}^{L}\sqrt{\gamma_i} \le \sqrt{(L+1)\gamma_{\text{th}}}\right) \\ &= P(r \le \widetilde{\gamma}_{\text{th}}), \end{aligned} \tag{49}$$

where $\widetilde{\gamma}_{\text{th}} = \sqrt{(L+1)\gamma_{\text{th}}}$.

Using Lemma 1, the outage probability in (49) can be given as

$$P_{\text{out}} = \frac{1}{2} - \frac{1}{\pi}\int_0^{\infty} \frac{\text{Im}\left[\phi_r(t)e^{-j\widetilde{\gamma}_{\text{th}}t}\right]}{t}dt. \tag{50}$$

Exploiting the polar form of CHF of r, we get the expression for the outage probability as

$$\begin{aligned} P_{\text{out}} = \frac{1}{2} &- \frac{\prod_{i=0}^{L}\Phi_i^*}{\pi} \\ &\times \int_0^{\infty} \prod_{i=0}^{L}\left[c_i^2(t) + d_i^2(t)\right]^{1/2} \\ &\times \sin\left(\sum_{i=0}^{L}\tan^{-1}\frac{d_i(t)}{c_i(t)} - \widetilde{\gamma}_{\text{th}}t\right)dt. \end{aligned} \tag{51}$$

For simpler numerical implementation, the outage probability can be expressed in one product-sum integral form. For instance, in case of $L = 1$, P_{out} is

$$\begin{aligned} P_{\text{out}} = \frac{1}{2} &- \frac{\Phi_0^*\Phi_1^*}{\pi} \\ &\times \int_0^{\infty} \frac{[\mathcal{A}]\cos\widetilde{\gamma}_{\text{th}}t - [c_0(t)c_1(t) - d_0(t)d_1(t)]\sin\widetilde{\gamma}_{\text{th}}t}{t}dt, \end{aligned} \tag{52}$$

where $\mathcal{A}$ denotes $[c_0(t)d_1(t) + c_1(t)d_0(t)]$. Similarly, for $L = 2$, P_{out} can be formulated as

$$\begin{aligned} P_{\text{out}} = \frac{1}{2} &- \frac{\Phi_0^*\Phi_1^*\Phi_2^*}{\pi} \\ &\times \int_0^{\infty} \{[c_0(t)c_1(t)d_2(t) + c_0(t)c_2(t)d_1(t) \\ &+ c_1(t)c_2(t)d_0(t) - d_0(t)d_1(t)d_2(t)]\cos\widetilde{\gamma}_{\text{th}}t \\ &- [c_0(t)c_1(t)c_2(t) - c_2(t)d_0(t)d_1(t) \\ &- c_1(t)d_1(t)d_2(t) - c_0(t)d_1(t)d_2(t)]\sin\widetilde{\gamma}_{\text{th}}t\}\frac{dt}{t}. \end{aligned} \tag{53}$$

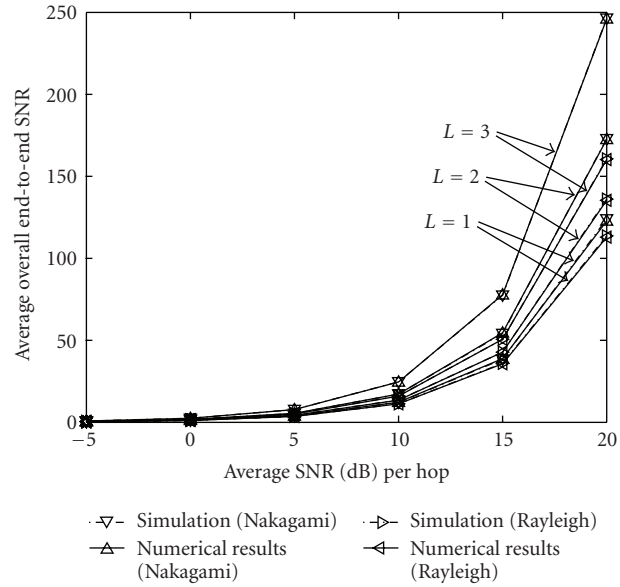

Figure 3: Average overall end-to-end SNR for $L = 1, 2$, and 3 in Rayleigh and Nakagami-m fading channels.

4. Numerical and Simulation Results

In order to verify the accuracy of the derived expressions, several numerical results and simulations are presented in this section. Each performance criterion is evaluated in two different fading environments. In the first case, we consider Rayleigh fading as a special case with $m_i = 1$ and $\gamma_i = \gamma$, for all $i = 0, \ldots, L$. In the other case, to illustrate diversity, Nakagami-m fading with different parameters for each branch is considered. In this situation, we assume $m_0 = 0.5$, $m_1 = 1.5$, $m_2 = 2$, and $m_3 = 2.5$ as fading parameters. The average SNR per hop for the direct link and the relaying branches is assumed to be $\overline{\gamma}_0 = \overline{\gamma}$, $\overline{\gamma}_1 = 1.2\overline{\gamma}$, $\overline{\gamma}_2 = 1.5\overline{\gamma}$ and $\overline{\gamma}_3 = 2\overline{\gamma}$.

Figure 3 shows the average overall end-to-end SNR versus the average SNR per hop in Rayleigh and Nakagami-m fading, respectively. First, we use (23) to obtain the average statistics of the moments of end-to-end SNR. Then, (24) is used to calculate the average overall end-to-end SNR. This figure proves that the analytical results presented for the average end-to-end SNR of a multibranch dual-hop relay system are very precise as the numerical results coincide with the simulation results in both fading environments.

In Figure 4, we illustrate the ABEP versus the average SNR per hop in Rayleigh fading environment for coherent BPSK and noncoherent DBPSK relay systems, respectively. Comparative curves using MRC are also shown. The analytical results for the ABEP of coherent modulation schemes are obtained by presenting the CHF of the total fading envelope r in product form and then taking the infinity range integrals such as (41) and (42). However, due to the complication of the integrand, it is difficult to take numerical integral over $(0, \infty)$. Fortunately, the integrand approaches zero as t approaches infinity. Hence, it is a converging integral. Therefore, instead of evaluating the integral over $(0, \infty)$,

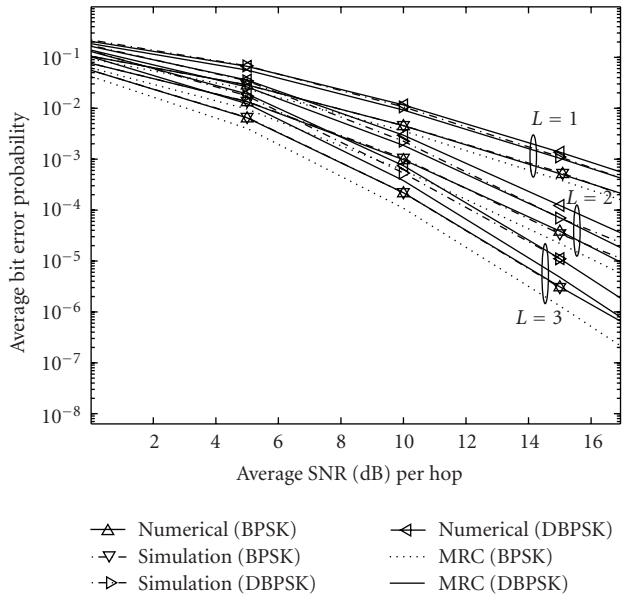

Figure 4: Average bit error probability for BPSK and DBPSK for $L = 1, 2$, and 3 using EGC and MRC in Rayleigh fading channels.

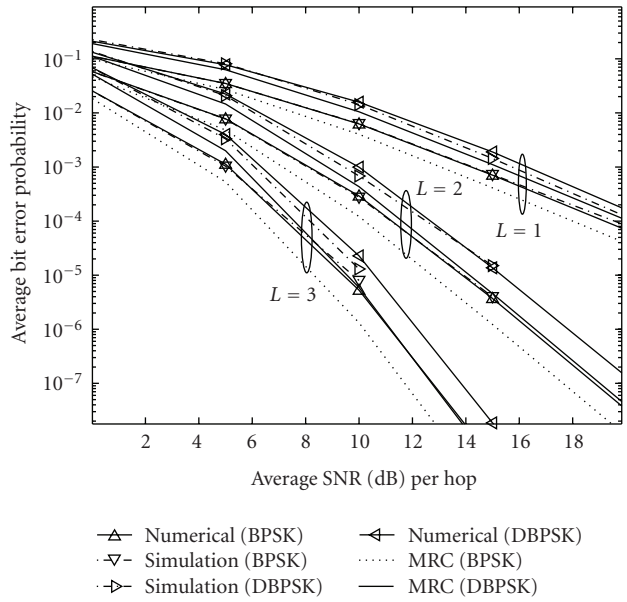

Figure 5: Average bit error probability for BPSK and DPSK for $L = 1, 2$, and 3 using EGC and MRC in Nakagami-m fading channels.

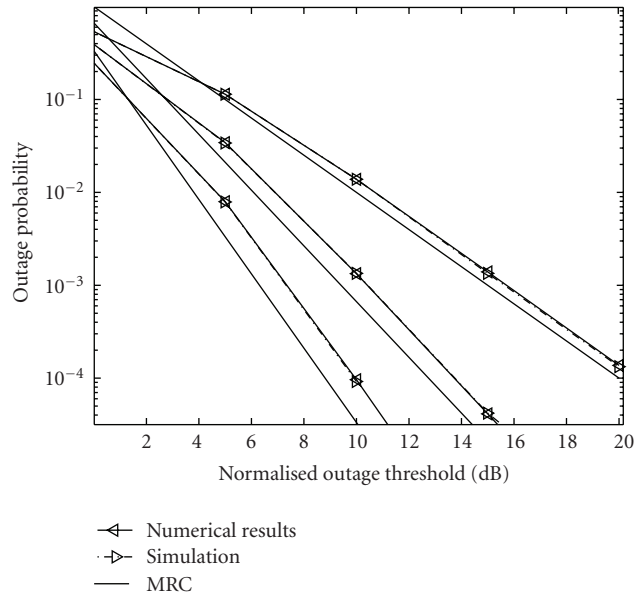

Figure 6: Outage probability for BPSK for $L = 1, 2$, and 3 using EGC and MRC in Rayleigh fading channels.

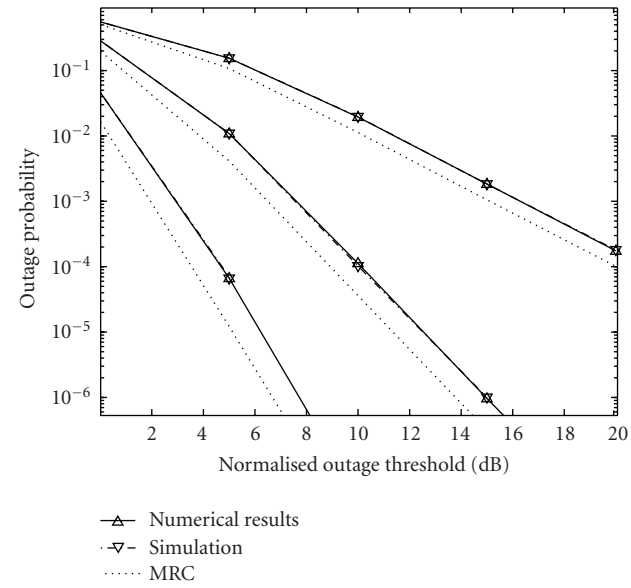

Figure 7: Outage probability for BPSK for $L = 1, 2$, and 3 using EGC and MRC in Nakagami-m fading channels.

we approximately evaluate it over $(0, t_{\max})$, where $t_{\max}$ is chosen so that the truncation of the integrand is as small as possible and the numerical value remains almost the same. However, the choice of $t_{\max}$ does not follow any hard and fast rule, rather it depends upon the system configuration. Despite this approximation, Figure 4 shows that the analytical results closely match the computer simulations in case of coherent BPSK, regardless of the number of branches. However, the simulation results for DBPSK follow the numerical ones with a very small difference for all SNR regions.

Figure 5 depicts the ABEP of the coherent BPSK and noncoherent DBPSK, respectively, in Nakagami-m fading channels with the parameters stated above. Comparative curves using MRC are also shown. A similar trend as in Rayleigh channels is also observed in Nakagami-m channels. It is emphasized here that when the values of m for all the considered branches are close together, the simple form of the overall SNR for EGC in (17) can be applied.

We also simulate P_{out} in order to testify the numerical result of (51). In Figures 6 and 7, we plot P_{out} versus the normalized outage threshold in Rayleigh and Nakagami-m

environments, respectively. It is evident that in both cases, the numerical results nearly coincide with the simulation results.

5. Conclusion

This paper investigated the performance of a multi-branch dual-hop non-regenerative relay system operating in Nakagami-m fading environment. We presented the PDF of the end-to-end SNR in terms of a special function called Meijer's G function. We then derived the closed form expressions for the moments of the overall SNR, the amount of fading, and the spectral efficiency. We obtained the analytical expressions for the average bit error probability and the outage probability for coherent and noncoherent modulation schemes using characteristic function approach. The obtained formulae are presented in only one-fold integral form which is simple to evaluate. The accuracy of these formulae is verified by extensive computer simulations.

Appendices

A. Derivation of PDF of Z_i

Let $s_{1i} = |h_{1i}|^2$ and $s_{2i} = |h_{2i}|^2$, then $z_i = s_{2i}/s_{1i}$. By using the PDF of $|h|$ in (3) and [25, Section 5-2], the PDFs of s_{1i} and s_{2i} are obtained as

$$p_{S_{ji}}\left(s_{ji}\right) = \frac{m_i^{m_i} s_{ji}^{m_i-1}}{\Omega_i^{m_i}\Gamma(m_i)} \exp\left(-\frac{m_i s_{ji}}{\Omega_i}\right) \quad j = 1, 2. \tag{A.1}$$

Now using [25, (6-43)] and (A.1), we can derive the PDF of Z_i as

$$\begin{aligned} p_{Z_i}(z_i) &= \int_0^\infty s_{1i} p_{S_{2i}}(z_i s_{1i}) p_{S_{1i}}(s_{1i}) ds_{1i} \\ &= \frac{m_i^{2m_i} z_i^{m_i-1}}{\Omega_i^{2m_i}\Gamma^2(m_i)} \int_0^\infty s_{1i}^{2m_i-1} \exp\left(-\frac{m_i}{\Omega_i}(1+z_i)s_{1i}\right) ds_{1i}. \end{aligned} \tag{A.2}$$

Using and simplifying [20, (3.381.4)], we obtain the PDF of Z_i as in (16). The moments of z_i are derived from its definition as

$$\begin{aligned} \mathbf{E}[z_i^n] &= \int_0^\infty z_i^n p_{Z_i}(z_i) dz_i \\ &= \frac{\Gamma(2m_i)}{\Gamma^2(m_i)} \int_0^\infty \frac{z_i^{m_i+n-1}}{(1+z_i)^{2m_i}} dz_i. \end{aligned} \tag{A.3}$$

Using [20, (3.194.3)] with constraint $m_i > n$, we obtain the moments of z_i as

$$\mathbf{E}[z_i^n] = \frac{\Gamma(2m_i)}{\gamma^2(m_i)} B(m_i + n, m_i - n), \tag{A.4}$$

where $B(\cdot,\cdot)$ is the Beta function defined in [20, (3.380)]. Using [20, (8.384.1)], we can further simplify the moments of z_i in terms of Gamma functions

$$\mathbf{E}[z_i^n] = \frac{\Gamma(m_i + n)\Gamma(m_i - n)}{\Gamma^2(m_i)}. \tag{A.5}$$

Utilizing the first and second moments of z_i, we get the average and the variance of z_i as

$$\begin{aligned} \mathbf{E}[z_i] &= \frac{m_i}{m_i - 1}, \quad \text{with } m_i > 1, \\ \text{var}(z_i) &= \frac{m_i(2m_i - 1)}{(m_i - 2)(m_i - 1)^2}, \quad \text{with } m_i > 2. \end{aligned} \tag{A.6}$$

B. The PDF of r_i

In [25, Section 5-2], it is shown that if a RV x has a PDF $p_X(x)$, then another RV y such that $y = \sqrt{x}$ has PDF as follows

$$p_Y(y) = \frac{p_X(y^2)}{\left|1/2\sqrt{y^2}\right|} = 2y p_X(y^2). \tag{B.1}$$

Applying the above equation, we derive the PFDs of $r_0 = \sqrt{\gamma_0}$ and $r_i = \sqrt{\gamma_i}$ as

$$\begin{aligned} p_{r_0}(r_0) &= 2A_0 r_0^{2m_0-1} \exp\left(-\frac{m_0}{\overline{\gamma}_0} r_0^2\right), \\ p_{r_i}(r_i) &= 2A_i r_i G_{1,2}^{2,0}\left(\lambda_i r_i^2 \,\middle|\, {m_i - 1/2 \atop m_i - 1, 2m_i - 1}\right). \end{aligned} \tag{B.2}$$

C. The CHF of r_i

The CHF of r_0 is calculated as

$$\begin{aligned} \phi_{r_0}(t) &= \int_0^\infty e^{jtr_0} p_{r_0}(r_0) dr_0 \\ &= 2A_0 \int_0^\infty r_0^{2m_0-1} e^{jtr_0} \exp\left(-\frac{m_0}{\overline{\gamma}_0} r_0^2\right) dr_0 \\ &= 2A_0\sqrt{\pi}\left[\int_0^\infty r_0^{2m_0-1} G_{0,2}^{1,0}\left(\frac{t^2 r_0^2}{4}\,\middle|\, {\cdot \atop 0, 1/2}\right) \right. \\ &\qquad \times G_{0,1}^{1,0}\left(\frac{m_0}{\overline{\gamma}_0} r_0^2 \,\middle|\, {\cdot \atop 0}\right) dr_0 \\ &\qquad + j\,\text{sign}(t) \int_0^\infty r_0^{2m_0-1} G_{0,2}^{1,0}\left(\frac{t^2 r_0^2}{4}\,\middle|\, {\cdot \atop 1/2, 0}\right) \\ &\qquad \left. \times G_{0,1}^{1,0}\left(\frac{m_0}{\overline{\gamma}_0} r_0^2 \,\middle|\, {\cdot \atop 0}\right) dr_0 \right]. \end{aligned} \tag{C.1}$$

By putting $z_0 = r_0^2$, the integrals are reduced to

$$\begin{aligned}\phi_{r_0}(t) = A_0\sqrt{\pi}\Bigg[&\int_0^\infty z_0^{m_0-1} G_{0,2}^{1,0}\left(\frac{t^2 z_0}{4}\,\middle|\,{}^{\cdot}_{0,1/2}\right) \\ &\times G_{0,1}^{1,0}\left(\frac{m_0}{\overline{\gamma}_0} z_0\,\middle|\,{}^{\cdot}_{0}\right) dz_0 \\ &+ j\,\mathrm{sign}(t)\int_0^\infty z_0^{m_0-1} G_{0,2}^{1,0}\left(\frac{t^2 z_0}{4}\,\middle|\,{}^{\cdot}_{1/2,0}\right) \\ &\times G_{0,1}^{1,0}\left(\frac{m_0}{\overline{\gamma}_0} z_0\,\middle|\,{}^{\cdot}_{0}\right) dz_0\Bigg] \\ = \frac{\sqrt{\pi}}{\Gamma(m_0)}\Bigg[&G_{1,2}^{1,1}\left(\frac{\overline{\gamma}_0 t^2}{4m_0}\,\middle|\,{}^{1-m_0}_{0,1/2}\right) \\ &+ j\,\mathrm{sign}(t) G_{1,2}^{1,1}\left(\frac{\overline{\gamma}_0 t^2}{4m_0}\,\middle|\,{}^{1-m_0}_{1/2,0}\right)\Bigg].\end{aligned} \tag{C.2}$$

Similarly the CHF of r_i can be derived as

$$\begin{aligned}\phi_{r_i}(t) &= 2A_i\int_0^\infty r_i e^{jtr_i} G_{1,2}^{2,0}\left(\lambda_i r_i^2\,|\,{}^{m_i-1/2}_{m_i-1,2m_i-1}\right) \\ &= 2A_i\Bigg[\int_0^\infty r_i\cos(tr_i) G_{1,2}^{2,0}\left(\lambda_i r_i^2\,|\,{}^{m_i-1/2}_{m_i-1,2m_i-1}\right) dr_i \\ &\quad + j\int_0^\infty r_i\sin(tr_i) G_{1,2}^{2,0}\left(\lambda_i r_i^2\,|\,{}^{m_i-1/2}_{m_i-1,2m_i-1}\right) dr_i\Bigg].\end{aligned} \tag{C.3}$$

By putting $z_i = r_i^2$ and using [22, (13)], the CHF of r_i can be written as

$$\begin{aligned}\phi_{r_i}(t) = A_i\sqrt{\pi}\Bigg[&\int_0^\infty G_{1,2}^{2,0}\left(\lambda_i z_i|{}^{m_i-1/2}_{m_i-1,2m_i-1}\right) \\ &\times G_{0,2}^{1,0}\left(\frac{t^2}{4} z_i\,\middle|\,{}^{\cdot}_{0,1/2}\right) dz_i \\ &+ j\,\mathrm{sign}(t)\int_0^\infty G_{1,2}^{2,0}\left(\lambda_i z_i|{}^{m_i-1/2}_{m_i-1,2m_i-1}\right) \\ &\times G_{0,2}^{1,0}\left(\frac{t^2}{4} z_i\,\middle|\,{}^{\cdot}_{1/2,0}\right) dz_i\Bigg] \\ = \frac{2\pi}{4^m\Gamma^2(m_i)}\Bigg[&G_{2,3}^{1,2}\left(\frac{t^2}{4\lambda_i}\,\middle|\,{}^{1-m_i,1-2m_i}_{0,1/2-m_i,1/2}\right) \\ &+ j\,\mathrm{sign}(t) G_{2,3}^{1,2}\left(\frac{t^2}{4\lambda_i}\,\middle|\,{}^{1-m_i,1-2m_i}_{1/2,1/2-m_i,0}\right)\Bigg].\end{aligned} \tag{C.4}$$

Acknowledgment

This work is partly supported by the Australian Research Council Discovery project DP0879401.

References

[1] J. N. Laneman, D. N. C. Tse, and G. W. Wornell, "Cooperative diversity in wireless networks: efficient protocols and outage behavior," *IEEE Transactions on Information Theory*, vol. 50, no. 12, pp. 3062–3080, 2004.

[2] A. Sendonaris, E. Erkip, and B. Aazhang, "User cooperation diversity—part II: implementation aspects and performance analysis," *IEEE Transactions on Communications*, vol. 51, no. 11, pp. 1939–1948, 2003.

[3] M. O. Hasna and M. S. Alouini, "End-to-end performance of transmission systems with relays over Rayleigh fading channels," *IEEE Transactions on Wireless Communications*, vol. 2, no. 6, pp. 1126–1131, 2003.

[4] T. A. Tsiftsis, G. K. Karagiannidis, and S. A. Kotsopoulos, "Dual-hop wireless communications with combined gain relays," *IEE Proceedings: Communications*, vol. 152, no. 5, pp. 528–532, 2005.

[5] M. O. Hasna and M. S. Alouini, "Harminic mean and end-to-end performance of transmission systems with relays," *IEEE Transactions on Communications*, vol. 52, no. 1, pp. 130–135, 2004.

[6] D. A. Zogas, G. K. Karagiannidis, N. C. Sagias, T. A. Tsiftsis, P. T. Mathiopoulos, and S. A. Kostopoulos, "Dual-hop wireless communications over nakagami fading," in *Proceedings of the IEEE Vehicular Technology Conference (VTC '04)*, vol. 4, pp. 2200–2204, May 2004.

[7] P. A. Anghel and M. Kaveh, "Exact symbol error probability of a cooperative network in a Rayleigh-fading environment," *IEEE Transactions on Wireless Communications*, vol. 3, no. 5, pp. 1416–1421, 2004.

[8] A. Ribeiro, X. Cai, and G. B. Giannakis, "Symbol error probabilities for general cooperative links," *IEEE Transactions on Wireless Communications*, vol. 4, no. 3, pp. 1264–1273, 2005.

[9] T. A. Tsiftsis, G. K. Karagiannidis, S. A. Kotsopoulos, and F.-N. Pavlidou, "BER analysis of collaborative dual-hop wireless transmissions," *Electronics Letters*, vol. 40, no. 11, pp. 679–681, 2004.

[10] N. C. Beaulieu, "An infinite series for the computation of the complementary probability distribution function of a sum of independent random variables and its application to the sum of Rayleigh random variables," *IEEE Transactions on Communications*, vol. 38, no. 9, pp. 1463–1474, 1990.

[11] N. C. Beaulieu and A. A. Abu-Dayya, "Analysis of equal gain diversity on nakagami fading channles," *IEEE Transactions on Communications*, vol. 39, no. 2, pp. 225–234, 1991.

[12] Q. T. Zhang, "Outage probability in cellular mobile radio due to nakagami signal and interferers with arbitrary paramters," *IEEE Transactions on Vehicular Technology*, vol. 45, no. 2, pp. 364–372, 1996.

[13] Q. T. Zhang, "Probability of error for equal-gain combiners over Rayleigh channels: some closed-form solutions," *IEEE Transactions on Communications*, vol. 45, no. 3, pp. 270–273, 1997.

[14] Q. T. Zhang, "A simple approach to probability of error for equal gain combiners over Rayleigh channels," *IEEE Transactions on Vehicular Technology*, vol. 48, no. 4, pp. 1151–1154, 1999.

[15] A. Annamalai, C. Tellambura, and V. K. Bhargava, "Equal gain diversity receiver performance in wireless channels," *IEEE Transactions on Communications*, vol. 48, no. 10, pp. 1732–1745, 2000.

[16] V. Ramanathan and A. Annamalai, "Analysis of equal gain diversity receiveers in correlated Rayleigh fading channels," *IEEE Communications Letters*, vol. 8, no. 6, pp. 362–364, 2004.

[17] G. K. Karagiannidis, "Moments-based approach to the performance analysis of equal gain diversity in Nakagami-m fading," *IEEE Transactions on Communications*, vol. 52, no. 5, pp. 685–690, 2004.

[18] D. A. Zogas, G. K. Karagiannidis, and S. A. Kotsopoulos, "Equal gain combining over nakagami-n (Rice) and Nakagami-q (Hoyt) generalized fading channels," *IEEE Transactions on Wireless Communications*, vol. 4, no. 2, pp. 374–379, 2005.

[19] M. K. Simon and M. S. Alouini, *Digital Communication over Fading Channels*, John Wiley & Sons, New York, NY, USA, 2nd edition, 2005.

[20] I. S. Gradshteyn and I. M. Ryzhik, *Table of Integrals, Series and Products*, Academic Press, New York, NY, USA, 5th edition, 1994.

[21] A. Erdelyi, W. Magnus, F. Oberherttinger, and F. Tricom, *Tables of Integral Transforms*, vol. 2, McGraw Hill, New York, NY, USA, 1954.

[22] V. S. Adamchik and O. I. Marichev, "Algorithm for calculating integrals of hypergeometric type functions and its realization in reduce system," in *Proceedings of the International Symposium on Symbolic and Algebraic Computation (ISSAC '90)*, pp. 212–224, 1990.

[23] N. C. Sagias, "Closed-form analysis of equal-gain diversity in wireless radio networks," *IEEE Transactions on Vehicular Technology*, vol. 56, no. 1, pp. 173–182, 2007.

[24] C. Tellambura and A. Annamalai, "Derivation of Craig's formula for gaussian probaility function," *Electronics Letters*, vol. 35, no. 17, pp. 1424–1425, 1999.

[25] A. Papoulis, *Probaility, Random Variables and Stochastic Processes*, McGraw Hill, New York, NY, USA, 3rd edition, 1991.